How Wrong Can You Be? Can a Simple Spreading Formula Be Used to Predict Worst-Case Underwater Sound Levels?

Alec J Duncan and Miles J G Parsons

Centre for Marine Science and Technology, Curtin University, Perth, Western Australia.

ABSTRACT

Several simple spreading laws have been proposed to allow estimates of underwater sound levels to be made without the complication of numerical modelling. Underwater acoustic propagation depends in an involved way on a number of geometric and environmental parameters, including source, receiver and water depth, and water column and seabed acoustic properties. As a result, there are many scenarios in which the use of these formulae lead to large errors. However, there would be a place for a formula that could provide an upper limit on received sound levels in a particular situation as this would enable sound sources that had a very low probability of posing an environmental hazard to be quickly eliminated from further consideration. Such a formula is proposed in this paper and its bounds of applicability are explored by comparison with numerical model results for several scenarios.

INTRODUCTION

Estimating underwater sound levels due to human activities such as seismic surveys, offshore construction, and port maintenance and construction has become a topic of considerable interest in recent years as concern about the environmental impacts of man-made underwater sound has increased.

Equation (1), the formula for estimating the received sound level, is deceptively simple.

$$L_r = L_s - TL \tag{1}$$

Here L_s is the source level, which may be in any one of a number of different units depending on the particular situation, for example dB re 1μPa rms @ 1m, dB re 1μPa peak @ 1m, dB re 1μPa^2.s @ 1m. Alternatively, for frequency dependent calculations, L_s could be a source spectral level with units of dB re 1μPa^2/Hz @ 1m or dB re 1μPa^2.s/Hz @ 1m.

L_r is the received level, and is in the same units as L_s, but without the "@ 1m", and TL is the transmission loss. Strictly, TL has units of dB re 1m, but the "re 1m" is hardly ever stated. Note that TL may be different depending on the units used for L_s and hence L_r. For example the transmission loss for peak pressure will in general be different from that for root mean square (rms) pressure.

Most cases of interest for environmental impact assessment involve broadband sources which emit sound over a wide range of frequencies and all three quantities in Equation (1) must be treated as frequency dependent.

Estimating L_s and its frequency dependence from measured data is itself a challenging problem, but this is not considered further in this paper which concentrates on the second term on the right hand side of Equation (1), the transmission loss.

Calculating transmission loss is complicated by its dependence on many different factors, including the horizontal separation of the source and receiver, their positions in the water column, the temperature and salinity profiles of the water column, the water depth, the slope and roughness of the seabed, the geology of the seabed, and the roughness of the sea surface.

Despite this complexity, a number of numerical underwater acoustic propagation codes are now available that can carry out these calculations and determine the transmission loss for a given situation. (See http://oalib.hlsresearch.com/ for a number of different programs of this type.)

The ready availability of high speed desktop computers makes it possible to carry out these computations for most situations of interest within a reasonable period of time, however the programs themselves are difficult to use and prone to error if the user doesn't have a good understanding of how they work and of the underlying physics. As a consequence, this type of modelling remains the preserve of the specialist.

It would therefore be very useful if there was a simple method of estimating a worst-case (minimum) transmission loss for a given situation that could be used by environmental consultants and/or regulators to ascertain whether there was sufficient likelihood of underwater noise being a problem to warrant proceeding to the relatively time consuming and expensive, but much more accurate process of numerical modelling.

The purpose of this paper is to propose such a method, and to test its validity against numerical models for several common scenarios.

TRANSMISSION LOSS FORMULAE

The computational requirements of numerical propagation modelling were a significant obstacle in the past, so it is not surprising that there have been a number of attempts to derive simple formulae that could provide transmission loss estimates. Several of these are given in Urick (1983) and Richardson, et. al. (1995) provides a useful summary.

Equation (2) is the well known formula for transmission loss due to spherical spreading with absorption, that applies at distances much larger than the source size, but small enough that the effects of boundary reflections and refraction are considered negligible.

$$TL = 20\log_{10}(r) + \alpha r \tag{2}$$

Here r is the slant range between source and receiver (m), and α is the frequency dependent absorption coefficient (dB/m) which can be calculated from a number of standard formulae (eg. Fisher and Simmons 1977, Thorp 1967).

Sound can be constrained vertically in the ocean by refraction by the vertical sound speed gradient, reflection from the sea surface or seabed, or some combination of these. When this happens the sound energy can continue to spread horizontally but can no longer spread vertically. This is known as cylindrical spreading. Urick (1983) gives the following formula for this situation:

$$TL = 10\log_{10}(r_h) + 10\log_{10}(r_t) + (\alpha + \alpha_L)r_h \tag{3}$$

where r_h is the horizontal separation (m) between source and receiver (assumed much larger than the depth of the duct containing the sound), r_t is the range (m) at which the sound propagation is assumed to transition from spherical to cylindrical spreading, and α_L is an additional attenuation term used to account for leakage of energy from the duct. In a shallow water duct bounded at the bottom by the seabed the appropriate choice of r_t depends on the seabed properties, and particularly on the seabed's critical grazing angle. This is because rays with grazing angles smaller than the critical angle will undergo almost perfect reflection from the seabed, whereas steeper rays will suffer significant reflection loss. Softer, less reflective seabeds have smaller critical angles, trapping a narrower wedge of rays and leading to larger values of r_t.

Marsh and Schulkin (1962) used an empirical approach based on a large number of measurements in order to derive a spreading law for shallow water. They proposed a spherical spreading formula at short ranges, a cylindrical spreading law at long ranges and a $15\log_{10}(r_h)$ loss at intermediate ranges. There are also frequency and seabed type dependent 'near-field anomaly' and attenuation terms to be taken into account. Details are given in Urick (1983).

It should be noted that the original reason for the introduction of these formulae was to provide a 'best estimate' of transmission loss for predicting the performance of sonar systems, which typically operate over a narrow band of frequencies. This is a somewhat different requirement to the purpose of this paper, which is to derive a formula that gives the lower limit of the transmission loss for a broadband acoustic source.

DEVELOPMENT OF PROPOSED METHOD

Spreading loss

The first stage in developing the proposed method is to obtain an "average" transmission loss based on a consideration of geometrical spreading of sound energy. The approach taken here is very similar to that used by Urick (1983, p152) to derive a transmission loss formula for sound propagating in a surface duct.

Consider a point source of sound operating for a finite length of time, and the geometry shown in Figure 1. Here it is assumed that all the sound energy passing through A_0, a portion of a spherical shell of radius r_0 and azimuthal extent ϕ centred on the source, will subsequently pass through A, a portion of a cylindrical shell of radius r and height h, with the same azimuthal extent, also centred on the source. The path by which the sound energy travels from A_0 to A is immaterial.

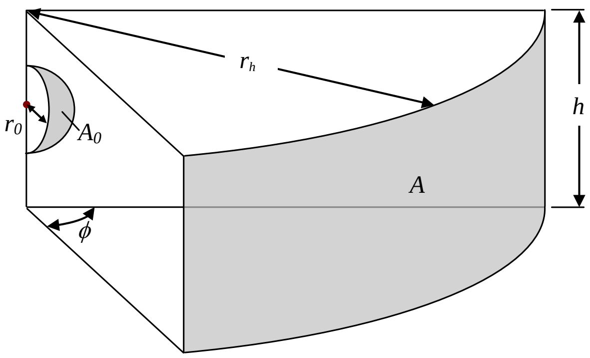

Figure 1. Geometry for deriving the proposed method.

Considering the average acoustic energy flux density (energy per square metre) passing through these two surfaces leads to the transmission loss for the average energy flux density:

$$\begin{aligned} TL_{\overline{E}} &= 10\log_{10}\left(\frac{\overline{E}_0}{\overline{E}}\right) \\ &= 10\log_{10}\left(\frac{A}{A_0}\right) \\ &= 10\log_{10}\left(\frac{r_h\phi h}{2r_0^2\phi}\right) \end{aligned}$$

which, with some rearrangement and adopting a reference distance, r_0, of 1m gives

$$TL_{\overline{E}} = 10\log_{10}(r_h) + 10\log_{10}\left(\frac{h}{2}\right) \tag{4}$$

where $\overline{E}_0$ is the average energy flux density through A_0 and $\overline{E}$ is the average energy flux density through A. Equation (4) is the same as Equation (3) with zero absorption and duct losses, and a transition distance of $r_t = h/2$. Note that the assumption made here that all of the energy passing through A_0 subsequently passes through A leads to a smaller transition distance, and hence lower transmission loss, than the often suggested value of $r_t = h$ (eg Richardson et. al. 1995). Equation (4) relates to the area averaged energy flux density and is therefore independent of the angular distribution of sound produced by the source.

Impulsive underwater sounds are most often characterised in terms of sound exposure level (SEL), which is the decibel representation of the integrated squared pressure, and is itself proportional to the energy density (acoustic energy per cubic metre). Sound crosses A_0 normal to the surface, so here the energy density is proportional to the energy flux density (energy per square metre crossing the surface in a given time). However, this is not the case at A where their relationship depends on the angular distribution of the sound, which is itself a function of the angular distribution of sound output by the source and the propagation conditions.

If the sound energy can be assumed to be travelling predominantly horizontally then the energy density and energy flux density are proportional and Equation (4) is an appropriate expression to use for the "average" transmission loss for SEL. (Here the averaging is understood to be carried out before converting to decibels.)

In a shallow water waveguide with a very reflective seabed there may be sufficient sound energy travelling at steep angles that the effect of non-horizontal propagation becomes significant. In the appendix it is shown that, in the case of an omnidirectional source in a shallow water waveguide with a perfectly reflecting seabed, Equation (4) would overestimate the transmission loss (leading to an underestimate of received level) by 2 dB. However, the results shown later indicate that, even for one of the most reflective seabeds likely to be encountered in practice (basalt), reflection losses appear to be sufficient to counteract this effect.

When considering the average intensity of sound from impulsive transient sources, some consideration must be given to the change in duration of the signal due to multipath propagation. This leads to a transmission loss for average intensity of:

$$TL_{\bar{I}} = TL_{\bar{E}} + 10\log_{10}\left(\frac{T}{T_0}\right) \tag{5}$$

where T_0 is the duration of the signal as it passes through A_0 and T is its duration as it passes through A. For a signal with a duration much longer than the time spread that occurs during propagation, $T/T_0 \approx 1$ and Equation (5) reduces to Equation (4). Even when this condition is not met, the effect of the temporal spreading term will be to increase the transmission loss, so using $T/T_0 = 1$ in Equation (5) is consistent with the aim of finding a lower bound for the transmission loss. The mean square pressure is proportional to the intensity, so Equation (5) is also appropriate for mean squared pressure levels (and root mean square (rms) pressure levels which are numerically equivalent).

Towards a lower limit

The formulae derived so far provide a lower limit for the transmission loss appropriate for the area averaged energy flux density and intensity. However, nothing in the derivation excludes the possibility that the energy may be unevenly distributed across area A, as a result of which the transmission loss appropriate for a particular receiver location may be lower than that predicted by equations (4) and (5). The pertinent question is, how much lower could it be?

In an attempt to answer that question, two main mechanisms for creating a spatially varying acoustic field are considered: 1. multipath (multimodal) interference, and 2. focusing effects due to refraction by the sound speed profile, reflection from the bathymetry, or both.

Interference effects

In most situations of practical interest for environmental impact assessments, sound travels from the source to the receiver via a number of paths of different lengths that may involve refraction by the sound speed gradient, reflection from the sea surface or seabed, and various combinations of these. The resulting interference leads to local increases and decreases in the intensity. (This discussion is phrased in terms of intensity, but is equally valid for the energy flux density).

Although difficult to quantify in general, the situation where there are many interfering ray paths with similar amplitude (or alternatively many interfering modes) leads to a simple result. In this case the Central Limit Theorem applies, the intensity conforms to an exponential probablility distribution and the pressure conforms to a Rayleigh distribution (Burdic 1984). The results of Shepherd and Milnarich (1973) can then be used to show that the probability of the intensity exceeding the mean intensity by y dB or more is given by:

$$p(I \geq y) = \exp[-\exp(0.23026y)] \tag{6}$$

Equation (6) is plotted in Figure 2. This result implies the following modification to (5) to account for these fluctuations:

$$TL_E = 10\log_{10}(r_h) + 10\log_{10}\left(\frac{h}{2}\right) - B \tag{7}$$

Here B is the threshold determined from Equation (6) or Figure(2) that gives an acceptable probability of exceedence. For example, a probability of exceedence of 0.01 would result in $B = 6.6$ dB.

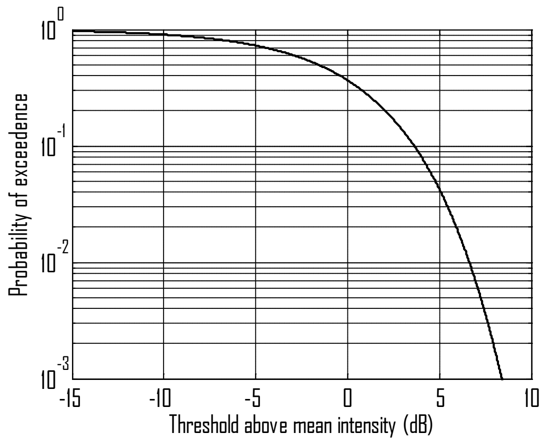

Figure 2. Probability of the intensity exceeding the mean intensity by at least the specified threshold assuming an underlying exponential intensity probability distribution (Rayleigh amplitude distribution).

The above discussion on interference pattern statistics applies when the source is emitting a continuous signal at a single frequency. Many sources of interest for environmental impact assessments emit sound over a wide band of frequencies, which has the effect of averaging out the statistical fluctuations in the signal amplitude to some extent. The degree to which this happens depends on the relationship between the bandwidth of the source and the frequency domain correlation properties of the interference field. The latter are difficult to determine in a simple way and so, in keeping with the aim of looking for a lower limit on the transmission loss, it is suggested that equations (6) and (7) be used as representing the worst case.

Focusing

Vertical-plane focusing of sound energy can occur due to refraction by the vertical sound speed profile, reflection from the seabed or sea surface, or some combination of these. Figure 3 shows the modelled transmission loss for a notional surface duct with a sound speed gradient of 0.2 ms^{-1}/m in the top 50m of the water column. This is a substantially steeper sound speed gradient than the value of 0.016 ms^{-1}/m expected for a well mixed surface layer (Medwin 1975) that is considered later in this paper, but serves to illustrate the point.

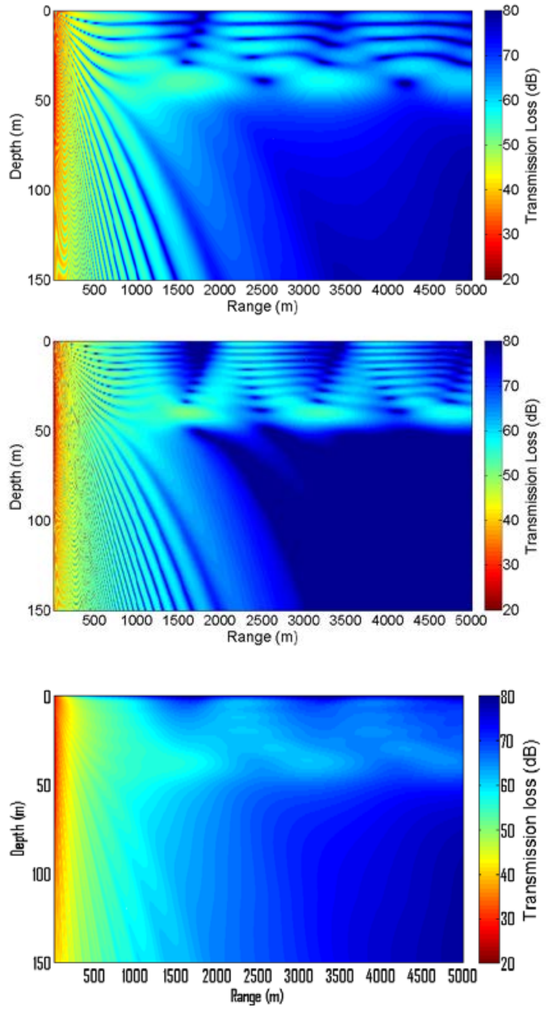

Figure 3. Transmission loss computed for a notional surface duct environment for frequencies of 1 kHz (top) and 2 kHz (middle). Bottom plot is incoherent average over 1/3 octave spaced frequencies from 100 Hz to 2 kHz. Source depth is 40m. Sound speed increases linearly from 1500ms^{-1} at the surface to 1510ms^{-1} at 50m depth, then decreases linearly to 1500ms^{-1} at 150m. The seabed has the same properties as the water column at 150m to simulate infinite depth. Propagation model is the SCOOTER fast-field model (Porter 2010).

The surface duct constrains the sound at the top by reflection from the sea surface and at the bottom by refraction. These processes combine to periodically refocus the sound energy at the source depth. Unlike the interference effects discussed above, which tend to average out over frequency, focusing is often largely frequency independent so that the resulting maxima will be just as significant for broad band sources as for narrowband. This effect is demonstrated in the lower plot in Figure 3, which plots the transmission loss incoherently averaged over 1/3 octave frequencies from 100 Hz to 2 kHz. The incoherent average is defined by:

$$TL_{inc} = -10\log_{10}\left(\frac{1}{N}\sum_{i=1}^{N}\left|p_i'\right|^2\right) \quad (8)$$

where $p_i' = 10^{-TL_i/20}$ is the received rms pressure relative to the transmitted rms pressure, and TL_i is the transmission loss at frequency i.

An example of focusing by reflection from the bathymetry is shown in Figure 4. In this example the sound speed is constant, but the curved seabed results in focusing of the sound energy in the upper part of the water column at a range of about 2000m.

In some cases the effect of reflections from the bathymetry and refraction is to constrain the sound energy to a smaller range of depths than would otherwise be the case, rather than focusing the sound on a small region. Figure 5 shows an example of this effect, in this case of downslope propagation into deep water. The bulk of the sound energy is refracted downward by the negative sound speed gradient and ends up concentrated in the lower half of the water column, leading to higher levels than would occur if it was uniformly spread.

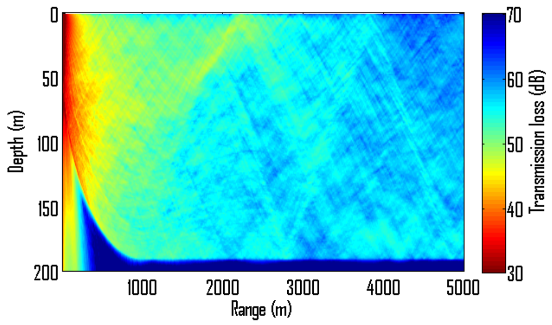

Figure 4. Incoherent average of transmission loss over 1/3 octave spaced frequencies from 100 Hz to 2 kHz, computed using RAMGeo (Collins 1993). Water column sound speed is independent of depth. The maximum in the upper part of the water column at a range of about 2000m is due to bathymetric focusing.

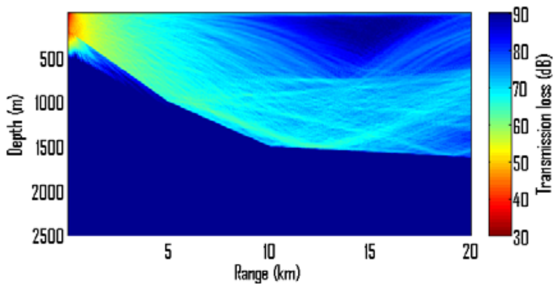

Figure 5. Incoherent average of transmission loss over 1/3 octave spaced frequencies from 100 Hz to 2 kHz, for downslope propagation with a notional deep water sound speed profile computed using RAMGeo (Collins 1993).

Although these examples are somewhat contrived, focusing effects are frequently encountered in practice, particularly in deep water. Figure 6 shows an example from a modelling exercise that was carried out as part of a study of possible environmental impacts of offshore seismic surveys. In this case the sound exposure levels have been estimated by calculating the transmission loss at many different frequencies, combining these with the source spectrum to obtain a received energy density spectrum, and then integrating over frequency. As discussed above, this procedure has the effect of averaging out the random fluctuations, but not the focusing effects, which in this case are due to a combination of reflection from the bathymetry and refraction.

A simple general criterion for a lower limit on transmission loss due to focusing is impractical due to the variety and complexity of the mechanisms. However, there are two situations in which these effects are unlikely to occur, and as a consequence, Equation (7) would be expected to be appropriate:

1. Well mixed water columns with flat seabeds.
2. Upslope propagation into shallow water.

The applicability of Equation (7) to these two situations will be investigated in the next section.

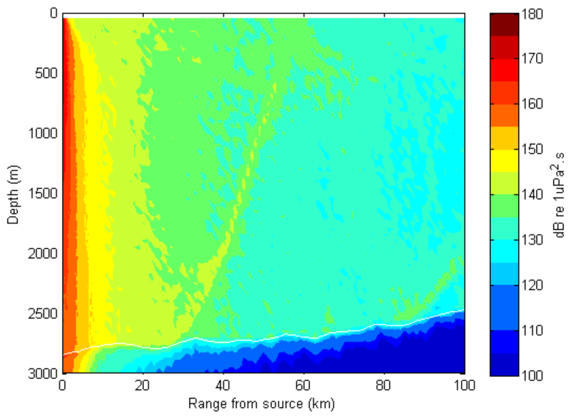

Figure 6. Example of a plot of modelled sound exposure level due to a broadband source (a seismic airgun array) in deep water.

TESTS OF APPLICABILITY

Well mixed water columns with flat seabeds

The top portion of the ocean is usually mixed by the action of surface waves and therefore has a fairly uniform temperature. As a result, this mixed layer has a sound speed profile that increases slightly with increasing depth at a rate of 0.016 ms^{-1}/m (Medwin 1975), and is therefore weakly upwardly refracting. The thickness of the mixed layer varies geographically and with present and past wave conditions, but it is typically between 25m and 200m (Pickard 1975). Providing the bathymetry is reasonably flat, focusing effects would be unlikely in this situation as propagation will be dominated by paths that involve multiple seabed and sea surface reflections.

The most reflective seabed likely to be encountered in practice is a hard rock such as basalt, which has the following typical acoustic properties (Jensen, 2000):

- Density, 2700 kgm^{-3}.
- Compressional wave sound speed, 5250 ms^{-1}.
- Shear sound speed, 2500 ms^{-1}
- Compressional wave attenuation, 0.1 dB/wavelemgth
- Shear wave attenuation, 0.2 dB/wavelength

A test case was created consisting of a 50m deep water column with a sound speed gradient of 0.016 ms^{-1}/m and a basalt seafloor. The transmission loss was calculated at 5 Hz intervals from 100 Hz to 1 kHz for a source depth of 30m using the fast field program SCOOTER. Figure 7 compares the minimum modelled transmission loss at any depth at 250 Hz, the minimum incoherently averaged transmission loss (averaged in 5 Hz steps from 100 Hz to 1 kHz), Equation (7) with B = 6.6 dB, and Equation (3) with a transition range equal to the water depth, which is often recommended. Note that this plot follows the usual convention of transmission loss increasing in the negative Y direction.

The results show that, except at ranges less than 50m where spherical spreading and near field interference effects are occurring, Equation (7) provides a good estimate of the lower bound on the 250 Hz transmission loss, and is a conservative lower bound on the incoherent transmission loss. Good agreement is obtained despite ignoring the expected 2 dB reduction in transmission loss due to the difference between energy density and energy flux density (see appendix). This implies that even for a highly refelctive basalt seabed there is enough reflection loss to counteract this effect.

By contrast the transmission loss predicted by Equation (3) is higher than the incoherent average, and this equation would therefore underpredict the received levels.

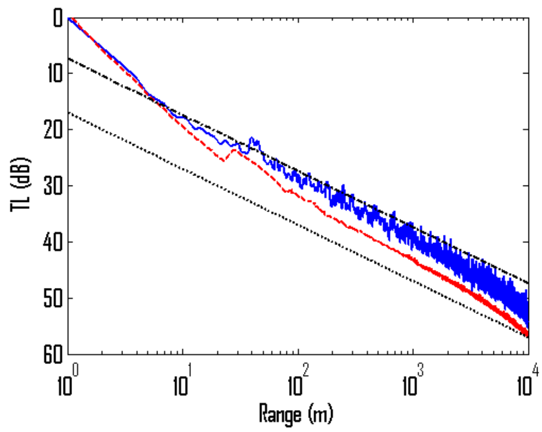

Figure 7. Comparison between transmission loss estimates for a 50m deep, isothermal water column with a flat basalt seabed. Source depth is 30m. Blue curve is minimum transmission loss at any depth at 250 Hz, red curve is minimum incoherent average transmission loss at any depth (5 Hz intervals from 100 Hz to 1 kHz), black dash-dot line is Equation (7) with B = 6.6 dB, and dotted line is Equation (3) with a transition range equal to the water depth and no attenuation.

Upslope propagation into shallow water

When sound sound travels up a slope, each successive seabed reflection steepens the ray paths, distributing the sound energy more evenly through the water column. As a result, Equation (7) would be expected to apply reasonably well sufficiently far upslope from the source. The scenario devised to test this involved propagation from a source located in 500m of water up a slope reminiscent of the top of the continental shelf. The sound speed profile was taken from ocean climatological data and is shown in Figure 8. It was desirable to use the parabolic equation model RAM to model this scenario, but as this program is unable to model shear wave effects a fluid seabed was used with the same density as basalt, but with a compressional wave velocity and attenuation equal to the shear wave properties of basalt given previously. This is a reasonably good approximation when the shear speed in the seabed is well in excess of the sound speed in the water.

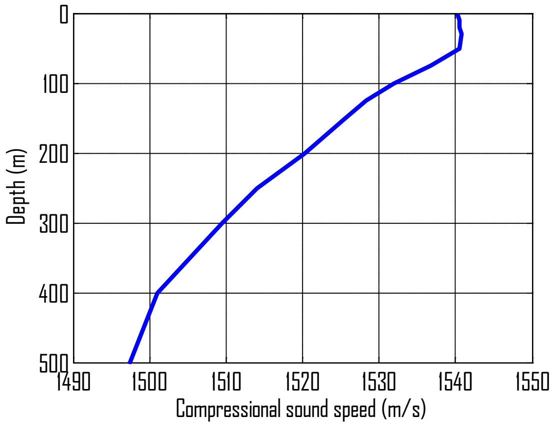

Figure 8. Sound speed profile used for the upslope test case.

Results were obtained for two different source depths, 10 m and 300 m. The 10 m results (Figures 9 and 10) show little evidence of focusing, even at short range, and the minimum transmission loss at 250 Hz at any depth in the water column stays above the value predicted by Equation (7) once the range exceeds 3 km.

The 300m source depth (Figures 11 and 12) gives rise to distinct focusing effects out to ranges in excess of 10 km, and in this case the minimum 250 Hz transmission loss doesn't stay above the value predicted by Equation (7) until the range exceeds 7 km.

Even with the focusing effects, Equation (7) is close to the lower limit on the 250 Hz transmission loss and provides a lower bound on the incoherent average at all ranges beyond about 200 m, whereas Equation (3) significantly overpredicts the transmission loss until the range exceeds approximately 20 km.

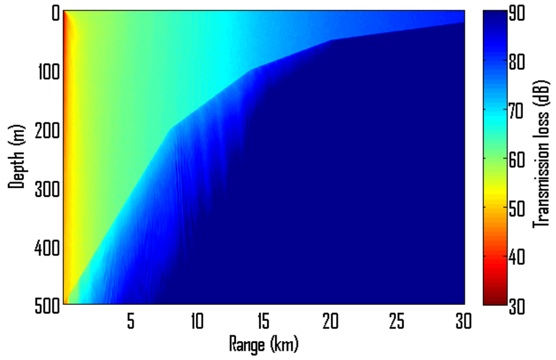

Figure 9. Transmission loss incoherently averaged from 100 Hz to 1 kHz in 5 Hz steps plotted as a function of range and depth for the upslope propagation example. Source depth is 10m.

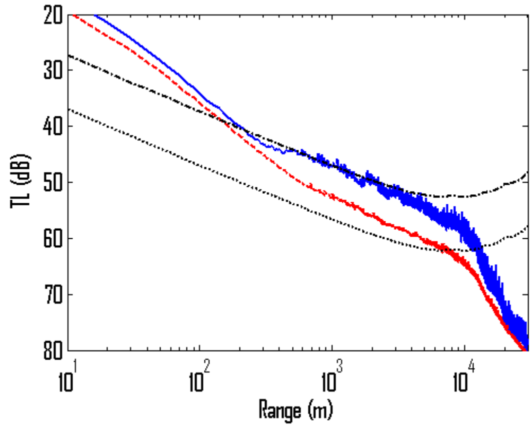

Figure 10. Comparison between transmission loss estimates for the upslope test case with a source depth of 10m. Blue: minimum transmission loss at any depth at 250 Hz. Red: minimum incoherent average transmission loss at any depth (5 Hz intervals from 100 Hz to 1 kHz). Black dash-dot: Equation (7) with B = 6.6 dB. Black dotted: Equation (3) with a transition range equal to the water depth and no attenuation.

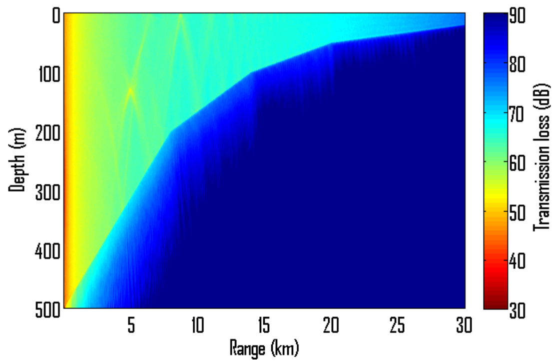

Figure 11. Transmission loss incoherently averaged from 100 Hz to 1 kHz in 5 Hz steps plotted as a function of range and depth for the upslope propagation test case. Source depth is 300m.

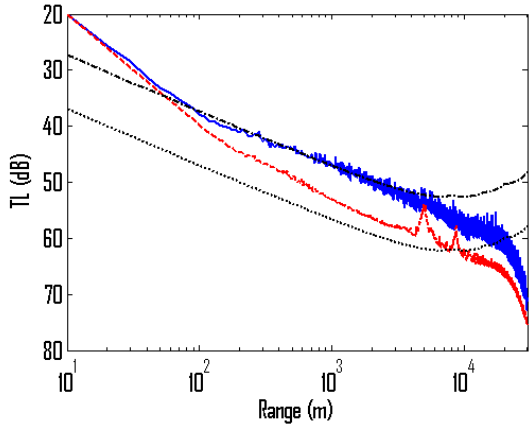

Figure 12. Comparison between transmission loss estimates for the upslope test case with a source depth of 300m. Blue: minimum transmission loss at any depth at 250 Hz. Red: minimum incoherent average transmission loss at any depth (5 Hz intervals from 100 Hz to 1 kHz). Black dash-dot: Equation (7) with B = 6.6 dB. Black dotted: Equation (3) with a transition range equal to the water depth and no attenuation.

CONCLUSIONS

The test cases used here demonstrate that the use of Equation (3) with a transition range equal to the water depth, as is often recommended, can lead to significant overestimates of the transmission loss and consequent underestimates of received levels.

However, it appears that Equation (7) with the allowance for interference effects, B = 6.6 dB, provides a useful lower bound on the transmission loss at least under the following circumstances:

- A shallow water waveguide with a reasonably flat seabed and a well mixed water column. In this case the equation is valid for ranges well in excess of the water depth.
- Upslope propagation into shallow water. In this case the equation is valid once the sound has travelled sufficiently far upslope for focussing effects to be largely eliminated by ray steepening.

Further work is requried to ensure that these preliminary conclusions apply to a wide range of similar scenarios, and also to further investigate whether it is possible to find a straightforward way of dealing with other common scenarios, such as downslope propagation.

APPENDIX: RELATIONSHIP BETWEEN ENERGY DENSITY AND ENERGY FLUX DENSITY FOR A SHALLOW WATER WAVEGUIDE WITH A PERFECTLY REFLECTING SEABED

One method of modelling acoustic propagation in an isovelocity, shallow water waveguide of constant depth is the method of images, which is described in a number of texts, including Brekhovskikh and Lysanov (2003), Section 5.1. The geometry is shown in Figure 13, which shows an infinite vertical line array of omnidirectional image sources that accounts for the the multiply reflected paths between the actual source and receiver. For a perfectly reflecting seabed and sea surface the contribution of each image source to the received signal is determined by spherical spreading.

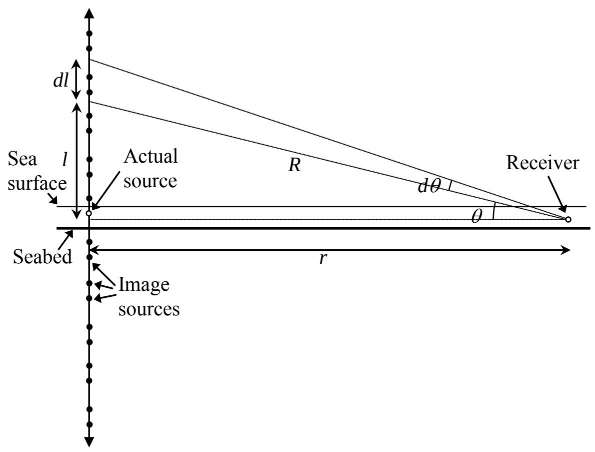

Figure 13. Geometry for applying the method of images to an isovelocity, shallow water waveguide.

If the separation between source and receiver is sufficiently large compared to an acoustic wavelength, fluctuations in the transmission path lengths caused by surface roughness and random inhomogeneities in the water column will randomise the signal phases at the receiver. In this case it is appropriate to calculate the received signal by an incoherent summation over the image sources, which is equivalent to summing the energy density contributed by each source.

To proceed further we approximate the line array of discrete sources shown in Figure 13 by a continuous line source that produces the same average energy density per unit length. This enables the energy density at the receiver to be calculated by the following integral:

$$D = \int_{-\infty}^{\infty} \frac{S}{R^2} dl \tag{A1}$$

where S is the acoustic energy density per unit length produced by the line source (assumed constant and independent of both position and angle), referred to a distance of 1m from the source element, and the other parameters are defined in Figure 13.

From Figure 13 it is apparent that $R = \frac{r}{\cos\theta}$ and $dl = \frac{r}{\cos^2\theta} d\theta$, allowing Equation (A1) to be written:

$$D = \frac{S}{r}\int_{-\pi/2}^{\pi/2} d\theta = \frac{\pi S}{r} \tag{A2}$$

The energy flux density through a surface in time T due to an impinging plane wave is given by:

$$E_\theta = cTD_\theta \cos\theta = \frac{cTS}{R^2}\cos\theta \tag{A3}$$

where D_θ is the energy density, c is the sound speed, and θ is the angle between the direction of travel of the plane wave and the normal to the surface. Although we are dealing here with spherical, rather than plane waves, this formula can still be used providing the receiver is sufficiently far from the source.

The total energy flux density is therefore given by:

$$E = \int_{-\infty}^{\infty} E_\theta dl = \int_{-\infty}^{\infty} \frac{cTS\cos\theta}{R^2} dl \tag{A4}$$

which, with the same substitutions used previously becomes:

$$E = \frac{cTS}{r}\int_{-\pi/2}^{\pi/2} \cos\theta d\theta = \frac{2cTS}{r} \tag{A5}$$

Converting this value to an energy density using the assumption that all energy is travelling horizontally (Equation (A3) with $\theta = 0°$) would result in:

$$D' = \frac{2S}{r} \tag{A6}$$

Comparing equations (A6) and (A2) it is apparent that the actual energy density exceeds that calculated under the usual assumption that all energy is travelling horizontally by a factor of $\pi/2$, or 1.96 dB.

The implication of this is that Equation (4) will overestimate the transmission loss (leading to an underestimate of received level) by about 2 dB for isovelocity shallow water waveguides with perfectly reflecting boundaries. This has been verified by the authors using numerical modelling with the SCOOTER fast-field model (Porter 2010).

It would be relatively straightforward to incorporate source directionality into this analysis by making S a function of θ. This has not been attempted, however the expectation is that the effect would be smaller for sources with their main beam oriented horizontally, and larger for sources that direct most of their energy downward or upward.

REFERENCES

Brekhovskikh, LM, and Lysanov, YP, 2003, *Fundamentals of ocean Acoustics*, Springer-Verlag, ISBN 0-387-95467-8.

Burdic, WS, 1984, *Underwater acoustic systems analysis*, Prentice-Hall, ISBN 0-13-936716-0.

Collins, MD, 1993, "A split-step Pade solution for the parabolic equation method", *J. Acous. Soc. America*, vol. 93, no. 4, pp. 1736-1742.

Fisher, FH and Simmons, VP, 1977, "Sound absorption in sea water", *J. Acous. Soc. America*, vol. 62, p. 558.

Jensen, FB, Kuperman, WA, Porter, MB, and Schmidt, H, 2000, *Computational Ocean Acoustics*, Springer, NY, ISBN 1-56396-209-8.

Marsh, HW and Schulkin, M, 1962, "Shallow water transmission loss", *J. Acous. Soc. America*, vol.34, p. 863.

Medwin, H, 1975, "Speed of sound in water: A simple equation for realistic parameters", *J. Acous. Soc. America*, vol. 58, no. 6, pp. 1318-1319.

Pickard, GL, 1975, *Descriptive physical oceanography*, Pergamon,

Porter, M. B., 2010, "Acoustics toolbox", http://oalib.hlsresearch.com/Modes/AcousticsToolbox/.

Thorp, WH, 1967, "Analytic description of the low frequency attenuation coefficient", *J. Acous. Soc. America*, vol. 42, p. 270.

Richardson WJ, Greene Jr, CR, Malme, CI, Thomson, DH, 1995, *Marine mammals and noise*, Academic Press, 0-12-588440-0.

Shepherd, WL and Milnarich Jr, P, 1973, "Basic relations between a Rayleigh-distributed randomly varying voltage and a decibel record of the voltage", Proceedings of the IEEE, pp. 1765-1766.

Urick, RJ, 1983, *Principles of underwater sound*, 2nd ed., Peninsula Publishing, ISBN 0-932146-62-7.